CHAPTER 2

Fundamentals of Non-linear Optics in Nanostructures

SERGEJS BOROVIKS* AND OLIVIER J. F. MARTIN*

Nanophotonics and Metrology Laboratory, Swiss Federal Institute of Technology Lausanne (EPFL), Switzerland
*Emails: sergejs.boroviks@epfl.ch; olivier.martin@epfl.ch

2.1 Introduction

Light plays a central role in the way we experience the world around us and this perception is solely based on linear optics.[1] For example, the rays with different colours forming a rainbow can be computed individually and then superposed without any interaction among them to form the complete shade of colours.[2] This means that all these phenomena can be described by the linear wave equation and the response of matter to incident light is merely linearly proportional to the electric field of the optical wave. Formally, the response of matter is called the polarization $\boldsymbol{P}$ and represents the density of dipole moments induced by the applied electric field $\boldsymbol{E}$ associated with the optical wave.[3] In linear optics, the polarization is linearly proportional to the field,

$$\boldsymbol{P}(\boldsymbol{r},t) = \varepsilon_0 \underline{\chi} \cdot \boldsymbol{E}(\boldsymbol{r},t), \tag{2.1}$$

where ε_0 is the vacuum permittivity and $\underline{\chi}$ the linear electric susceptibility, and we have assumed an infinite homogeneous material.[4] We use the metre kilogram second ampere (MKSA) unit system throughout this chapter and consider non-magnetic materials [in which the relative permeability $(\mu_r) = 1$].

Optical, Electronic and Magnetic Materials No. 2
Laser-based Techniques for Nanomaterials: Processing to Characterization
Edited by Nandakumar Kalarikkal, Rodolphe Antoine, Sabu Thomas and Padiyakkuth Nideesh

Published by the Royal Society of Chemistry, www.rsc.org

In our previous example of a rainbow, the water droplets are isotropic and the linear susceptibility χ is a scalar, which one often relates to the relative permittivity ε_r or to the refractive index n of the medium through the relation

$$\chi = \varepsilon_r - 1 = n^2 - 1. \tag{2.2}$$

However, in eqn (2.1), we emphasize that in the general case of an anisotropic medium, the susceptibility $\underline{\chi}$ is a rank 2 tensor, *i.e.* a 3×3 matrix.[5] Anisotropy plays a key role in non-linear optics, as will be discussed in the following paragraphs.

The linear eqn (2.1) is valid for small applied optical fields $\boldsymbol{E}(\boldsymbol{r}, t)$, such as those produced by most optical sources. When the applied field becomes comparable to the interatomic electric field,[6,7] 10^5–10^8 V m^{-1}, linear optics is not sufficient anymore to describe light–matter interactions and additional terms must be included in eqn (2.1):

$$\boldsymbol{P}(\boldsymbol{r}, t) = \varepsilon_0 \left(\underline{\chi} \cdot \boldsymbol{E}(\boldsymbol{r}, t) + \underline{\underline{\chi}}^{(2)} : \boldsymbol{E}(\boldsymbol{r}, t)\boldsymbol{E}(\boldsymbol{r}, t) + \underline{\underline{\underline{\chi}}}^{(3)} : \boldsymbol{E}(\boldsymbol{r}, t)\boldsymbol{E}(\boldsymbol{r}, t)\boldsymbol{E}(\boldsymbol{r}, t) \right). \tag{2.3}$$

The second-order susceptibility $\underline{\underline{\chi}}^{(2)}$ is a rank 3 tensor, while the third-order susceptibility $\underline{\underline{\underline{\chi}}}^{(3)}$ is a rank 4 tensor and ":" denotes the inner product.[5] Eqn (2.3) can be understood as a Taylor expansion of the polarization as a function of the applied field $\boldsymbol{E}(\boldsymbol{r}, t)$. The susceptibility tensors may have complex values, with the imaginary parts usually accounting for losses. To simplify the discussion, we will however assume real-valued susceptibilities in this section, however we will touch upon the importance of complex-valued susceptibilities when discussing non-linear absorption in Section 2.5.2.

For a vanishing applied field, the polarization also vanishes; for a small excitation field, the response of matter is linear with the field, while it becomes non-linear as the field increases. The three terms in eqn (2.3) are illustrated in Figure 2.1.

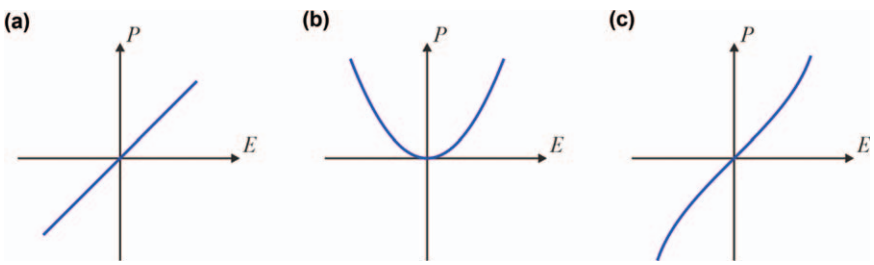

Figure 2.1 Illustration of the different polarization responses P of matter for a given applied field E included in eqn (2.3): (a) linear, (b) second order or quadratic, and (c) third order polarizations.

As is customary in a Taylor series, the different susceptibilities in eqn (2.3) decrease with their order:[8] the magnitude of the linear susceptibility $\underline{\chi}$ is in the order of unity as also evident from eqn (2.2) and does not have any units, whereas higher-order susceptibilities have magnitudes $\underline{\underline{\chi}}^{(2)} \sim 10^{-12}\mathrm{m\,V^{-1}}$ and $\underline{\underline{\underline{\chi}}}^{(3)} \sim 10^{-24}\mathrm{m^2\,V^{-2}}$, which indeed decrease dramatically with the order.[8]

One may therefore wonder why is it necessary to consider third-order non-linear effects since they are significantly smaller than second-order ones, even after multiplication of a higher power of the electric field? The main reason for that is the symmetry of the non-linear material, which can prevent second-order effects, whilst allowing third-order ones.

This is illustrated in Figure 2.2, where we show the second-order polarization response P as a function of the applied optical field E at the top and a centrosymmetric crystal with its atoms marked as black dots, and the centre of symmetry as a red dot at the bottom. In such a centrosymmetric crystal, the applied electric field changes the sign under the inversion operation: $E(-x_1) = -E(x_1)$, as illustrated by the black arrows pointing in the opposite directions. Conversely, the second-order non-linear polarization, which obeys quadratic dependence on the electric field, must not change sign upon inversion: $P(x_1) = P(-x_1)$, as shown by the blue arrows pointing in the same direction. This, however, is in contradiction with the crystal symmetry constraints, which imply that the second-order non-linear polarization should also change sign under inversion, *i.e.* $P(-x_1) = -P(x_1)$. The only way to reconcile this contradiction is to infer that the non-linear polarization vanishes, *i.e.* $P(x_1) = P(-x_1) = 0$. Hence, second-order non-linear processes do not exist in the bulk of a centrosymmetric crystal. Note that the previous discussion holds only when one considers the dipolar response of matter, which forms the basis for deriving the macroscopic theory of dielectric media,[9] whereas we review other possibilities of second-order responses in centrosymmetric material in Sections 2.4 and 2.5.

To conclude this brief introduction, we would like to mention that there are some comprehensive textbooks, where the topic of non-linear optics is treated in great detail.[10–13]

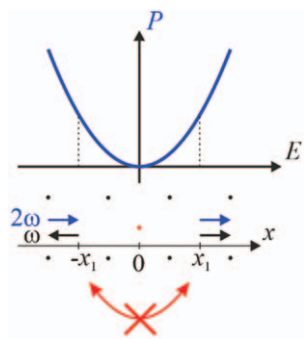

Figure 2.2 Illustration of the inexistence of SHG in a centrosymmetric system, see text for details.

2.2 Non-linear Wave Equation

Assuming an infinite homogeneous, non-magnetic, isotropic material, we can derive from Maxwell's equations the linear wave equation for the electric field $\boldsymbol{E}(\boldsymbol{r}, t)$ propagating in this medium:[4]

$$\nabla^2 \boldsymbol{E}(\boldsymbol{r}, t) - \frac{1}{c^2} \frac{\partial^2 \boldsymbol{E}(\boldsymbol{r}, t)}{\partial t^2} = 0, \tag{2.4}$$

where c is the speed of light in this medium. It is interesting to note that eqn (2.4) is a homogeneous equation without any source term; furthermore this equation is linear [the principle of superposition applies and if $\boldsymbol{E}_1(\boldsymbol{r}, t)$ and $\boldsymbol{E}_2(\boldsymbol{r}, t)$ are two independent solutions of the wave equation, then $\boldsymbol{E}_3(\boldsymbol{r}, t) = \boldsymbol{E}_1(\boldsymbol{r}, t) + \boldsymbol{E}_2(\boldsymbol{r}, t)$ is also a solution]; eqn (2.4) is therefore not fit to handle non-linear optical effects. A general non-linear wave equation that would apply to any physical system and be able to account for materials' properties, such as anisotropy, is extremely difficult to derive. To gain insights into the non-linear response of matter, one still usually assumes homogeneous and isotropic dielectric media, leading to the non-linear wave equation,[13]

$$\nabla^2 \boldsymbol{E}(\boldsymbol{r}, t) - \mu_0 \frac{\partial^2 \boldsymbol{D}(\boldsymbol{r}, t)}{\partial t^2} = \mu_0 \frac{\partial^2 \boldsymbol{P}_{\mathrm{nl}}(\boldsymbol{r}, t)}{\partial t^2}, \tag{2.5}$$

where μ_0 is the vacuum permeability and we have used the relation $c^2 = (\varepsilon_0 \mu_0 \varepsilon_{\mathrm{r}})^{-1}$ (we remind readers that we are considering non-magnetic materials). In eqn (2.5) we have introduced the displacement, $\boldsymbol{D}(\boldsymbol{r}, t) = \varepsilon_0 (\boldsymbol{E}(\boldsymbol{r}, t) + \underline{\chi} \cdot \boldsymbol{E}(\boldsymbol{r}, t))$, which accounts for the linear response of the system, while $\boldsymbol{P}_{\mathrm{nl}}(\boldsymbol{r}, t)$ is the non-linear response of matter:

$$\boldsymbol{P}_{\mathrm{nl}}(\boldsymbol{r}, t) = \varepsilon_0 \left(\underline{\underline{\chi}}^{(2)} : \boldsymbol{E}(\boldsymbol{r}, t)\boldsymbol{E}(\boldsymbol{r}, t) + \underline{\underline{\underline{\chi}}}^{(3)} : \boldsymbol{E}(\boldsymbol{r}, t)\boldsymbol{E}(\boldsymbol{r}, t)\boldsymbol{E}(\boldsymbol{r}, t) \right). \tag{2.6}$$

We note in eqn (2.5) that the non-linear response appears as the source term in that inhomogeneous equation. Furthermore, the optical field $\boldsymbol{E}$ is on both sides of eqn (2.5), making it self-consistent. Keeping in mind that we are dealing with non-linear phenomena, it is interesting to decompose the solution of this equation in a series of successive solutions in what is known as a Born series:[14] assuming that the initial field is monochromatic at frequency ω, the source term in eqn (2.5) produces one or several new frequencies through its non-linear response, *e.g.* ω', which was not present in the initial field. Solving the wave equation gives an electric field that contains these two frequencies ω and ω' that will also appear in the new source term in eqn (2.5), which may lead to additional frequencies in the non-linear response of the system. Overall, this phenomenon repeats, producing a plethora of interesting physical effects that are outlined in the next section.

2.3 Overview of Non-linear Phenomena

Guided by eqn (2.3), let us discuss separately second and third order non-linearities. This is best done in the frequency domain by considering harmonic optical fields with an $\exp(+j\omega t)$ temporal dependence. Furthermore, from now on we will assume scalar optical fields $\tilde{E}(\omega,t)=\tilde{E}(\omega)\exp(j\omega t)$, where the tilde symbol is introduced to emphasize that we are dealing here with complex values. Consequently, the physical optical field is given by the real part of the complex field:

$$E(\omega,t)=\Re[\tilde{E}(\omega,t)]=\frac{1}{2}[\tilde{E}(\omega)\exp(j\omega t)+\tilde{E}^{*}(\omega)\exp(-j\omega t)], \tag{2.7}$$

where the complex conjugate has been used for the last term. Furthermore, we will remove any tensorial dependence in the susceptibilities to simplify the following developments; the interested reader will find an extensive discussion of tensorial effects in Boyd (2020).[13]

2.3.1 Second-order Non-linear Phenomena

Let us consider the second-order term in eqn (2.6) for the non-linear response of matter: $P_{\mathrm{nl}}(\omega,t)=\varepsilon_0\chi^{(2)}E^2(\omega,t)$. Introducing eqn (2.7) in the non-linear response leads to a constant term plus a term at 2ω:

$$P_{\mathrm{nl}}(\omega,t)=P_{\mathrm{nl}}(0)+\Re[\tilde{P}_{\mathrm{nl}}(2\omega)\exp(j2\omega t)], \tag{2.8}$$

with

$$P_{\mathrm{nl}}(0)=\frac{1}{2}\varepsilon_0\chi^{(2)}\tilde{E}(\omega)\tilde{E}^{*}(\omega) \tag{2.9}$$

a time independent term that is proportional to the intensity of the incident optical field, while the second term reads

$$\tilde{P}_{\mathrm{nl}}(2\omega)=\frac{1}{2}\varepsilon_0\chi^{(2)}\tilde{E}^{2}(\omega). \tag{2.10}$$

Eqn (2.8) indicates that light at the new frequency 2ω has been created through the non-linear process, so-called second harmonic generation (SHG). Keeping in mind that this process is very weak, light at the fundamental frequency ω remains dominant in the system, as illustrated in Figure 2.3. We also note the appearance of the DC term, which corresponds to the generation of a constant polarization density in the non-linear medium, resulting into a DC voltage across this medium. This effect, which is called optical rectification, does not produce an optical field but rather a static voltage across the medium,[15] which can also damage the material under test and is very relevant for the topic of this book.[16]

The SHG intensity depends on the square of the interaction length l between the incident light and the material, and on the light intensity. Strong

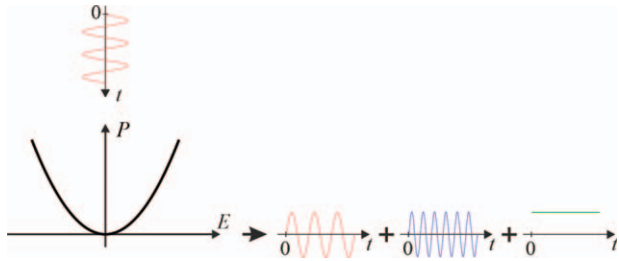

Figure 2.3 When a second order material is illuminated by a harmonic electric field at frequency ω (shown in red), light at the second harmonic 2ω is generated (shown in blue), as well as a DC field (shown in green). This SHG process is weak and most of the transmitted light remains at the fundamental frequency ω.

SHG requires therefore maximizing one or the other. We outline methods for SHG enhancement in Section 2.6.

We now turn to so-called three-wave mixing process by considering a polychromatic incident field with two frequencies ω_1 and ω_2, described as

$$E(\omega_1, \omega_2, t) = \Re[\tilde{E}_1(\omega_1)\exp(j\omega_1 t) + \tilde{E}_2(\omega_2)\exp(j\omega_2 t)]. \tag{2.11}$$

For such an illumination, the second-order non-linear response of the system will now include five terms at five different frequencies. First,

$$P_{\mathrm{nl}}(0) = \frac{1}{2}\varepsilon_0\chi^{(2)}(\tilde{E}_1(\omega_1)\tilde{E}_1^*(\omega_1) + \tilde{E}_2(\omega_2)\tilde{E}_2^*(\omega_2)), \tag{2.12}$$

which corresponds to a constant ($\omega = 0$) term, so-called optical rectification, similar to that in eqn (2.9). Then, two SHG terms at ω_1:

$$\tilde{P}_{\mathrm{nl}}(2\omega_1) = \frac{1}{2}\varepsilon_0\chi^{(2)}\tilde{E}_1{}^2(\omega_1), \tag{2.13}$$

and ω_2:

$$\tilde{P}_{\mathrm{nl}}(2\omega_2) = \frac{1}{2}\varepsilon_0\chi^{(2)}\tilde{E}_2{}^2(\omega_2). \tag{2.14}$$

Also, finally, there are two terms that depend on the sum of the illumination frequencies,

$$\tilde{P}_{\mathrm{nl}}(\omega_1 + \omega_2) = \varepsilon_0\chi^{(2)}\tilde{E}_1(\omega_1)\tilde{E}_2(\omega_2), \tag{2.15}$$

and on their difference,

$$\tilde{P}_{\mathrm{nl}}(\omega_1 - \omega_2) = \varepsilon_0\chi^{(2)}\tilde{E}_1(\omega_1)\tilde{E}_2^*(\omega_2). \tag{2.16}$$

These different processes are illustrated in Figure 2.4, where we introduce a description similar to the Jablonski diagrams used in fluorescence,[17]

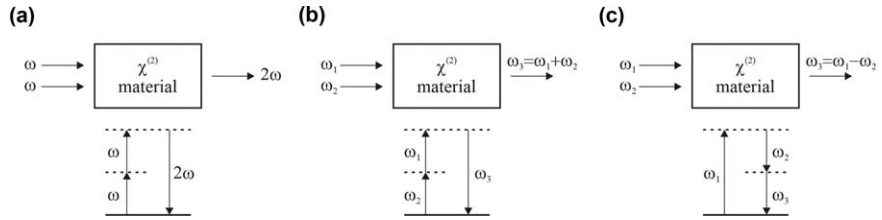

Figure 2.4 The different three-wave mixing phenomena that can occur in a second order non-linear material: (a) second harmonic generation (SHG), (b) sum frequency generation (SFG), and (c) difference frequency generation (DFG). Optical rectification, which produces a constant ($\omega = 0$) field is not shown. In the energy level description, the dashed lines correspond to virtual levels.

although, in the case of harmonic generation, the intermediate energy level is not a real, but a virtual level.

The phenomenon of three-wave mixing forms the basis for many important parametric processes, such as optical frequency conversion (the incident waves ω_1 and ω_2 are mixed to generate a wave $\omega_3 = \omega_1 + \omega_2$), optical parametric amplification (the wave ω_1 is amplified through a pump wave ω_3, while an idler wave ω_2 is created) and spontaneous parametric down conversion (the material is pumped with ω_3 and two waves with frequencies ω_1 and ω_2 are generated).

While three-wave mixing finds many important applications, we must point out that it is quite difficult to achieve with an arbitrary material, due to the prevalence of the dispersion, *i.e.* the frequency-dependent response of a material, which prevents achievement of the so-called phase matching condition. If we consider for example sum frequency, with $\omega_3 = \omega_1 + \omega_2$, which gives the matching condition for the waves' energies, we must also fulfil a similar condition for the momenta of these three waves:

$$\boldsymbol{k}_3 = \boldsymbol{k}_1 + \boldsymbol{k}_2. \tag{2.17}$$

Eqn (2.17) indicates that the phases of the three waves must advance concomitantly to sustain the generation of the new wave at frequency ω_3 from the original waves at ω_1 and ω_2. Keeping in mind that $k = \omega n/c_0$, with c_0 the speed of light in vacuum and n the refractive index at the corresponding frequency ω, one notes that fulfilling eqn (2.17) in a dispersive material is far from trivial and can only be achieved by taking advantage of the different refractive indices available in an anisotropic crystals.[12] We will see in Section 2.4 that this phase matching constraint can be alleviated in specific nanostructures.

2.3.2 Third-order Non-linear Phenomena

Let us consider the third order term in eqn (2.16) for the non-linear response of matter: $P_{\mathrm{nl}}(\omega, t) = \varepsilon_0 \chi^{(3)} E^3(\omega, t)$, where we have again neglected the vectorial

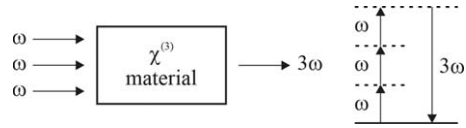

Figure 2.5 Illustration of third harmonic generation in a $\chi^{(3)}$ material.

character of the electric field and the tensorial nature of the susceptibility. Following what was done for second order processes, we could now study four-wave mixing by considering a polychromatic illumination with waves at the frequencies ω_1, ω_2 and ω_3, which will produce a response of the matter at 22 different frequencies, including, for example ${\omega_1}^3$, $\omega_1+\omega_2+\omega_3$, $\omega_1+\omega_2-\omega_3$, $2\omega_1+\omega_2$, $2\omega_3-\omega_3$, and so on. We will however limit our discussion to the simpler case where the three incident waves are at frequency ω and the generated wave at frequency 3ω, the so-called third-harmonic generation, illustrated in Figure 2.5.

Using a similar approach as for SHG, we obtain the following two terms for the third-order non-linear polarization response:

$$P_{\mathrm{nl}}(\omega,t)=\Re[\tilde{P}_{\mathrm{nl}}(\omega)\exp(j\omega t)+\tilde{P}_{\mathrm{nl}}(3\omega)\exp(j3\omega t)], \tag{2.18}$$

with

$$\tilde{P}_{\mathrm{nl}}(\omega)=\frac{3}{4}\varepsilon_0\chi^{(3)}|\tilde{E}(\omega)|^2\tilde{E}(\omega), \tag{2.19}$$

and

$$\tilde{P}_{\mathrm{nl}}(3\omega)=\frac{1}{4}\varepsilon_0\chi^{(3)}\tilde{E}^3(\omega). \tag{2.20}$$

The first term in eqn (2.19), which contains the non-linear susceptibility and the field intensity is often viewed as a field-dependant material, which susceptibility changes with the intensity of the applied field. This effect, known as optical Kerr effect,[13,18] can be used to control light with light, *e.g.* for switching or self-focusing.[19] In Section 2.5.2, we will see that other important processes that occur in nanostructures, such as two-photon absorption, stem from the third-order non-linear response of matter.

2.4 Surface Non-linear Effects

The surface contributions to the even-order non-linear effects are of particular importance, since, within the dipole approximation, they occur only in non-centrosymmetric systems.[13] In turn, a surface contribution to the odd-order effects was also reported,[20] although it may be generally considered as negligible.[21] In this section we focus on second-order surface non-linearities, which have remained within the scope of non-linear optics research for more than half a century.[22]

In principle, the surface of any material possesses a non-zero surface-normal component for the second-order susceptibility tensor, since the inversion symmetry (centrosymmetry) is naturally broken at the interface between two optically different materials.[23–25] This fact was first demonstrated experimentally in 1962 by Terhune *et al. via* SHG from a surface of calcite,[26] which is a centrosymmetric crystal. A few years later, Brown *et al.* reported SHG in reflection from the surface of a silver mirror,[27] whereas Bloembergen *et al.* demonstrated that this phenomenon is present at the surfaces of other metals, as well as semiconductors.[28] In recent years, SHG from noble metals has attracted particular interest, as it supports surface plasmon (SP) resonances.[29] SPs – delocalized electron oscillations at metal–dielectric interfaces – allow concentration of light in regions smaller than the diffraction limit[30] and thus are associated with the significant enhancement and gradients of the electric field across the metal–dielectric interfaces that lead to the amplification of non-linear optical processes.[13,31,32] Furthermore, it was recently shown that a strong electric field gradient itself may even increase the breakage of the symmetry at the surfaces of a plasmonic cavity made of centrosymmetric materials.[33]

There are two principal types of SP's: the surface plasmon polariton (SPP)[34] – an electromagnetic mode that propagates along a metal–dielectric interface – and localized surface plasmon (LSP)[35] – a mode confined to the surface of subwavelength-sized metal particle in a dielectric environment. Both SPP and LSP can be used for the enhancement of weak non-linearities at the interface between centrosymmetric metals and dielectrics. The first demonstration of the surface plasmon-enhanced optical SHG from a thin silver film[36] was reported by Simon *et al.* in 1974, whereas a plethora of both propagating and localized plasmon-enhanced non-linear systems are described in recent reviews.[22,37–40]

Generally, the non-linear surface polarization at frequency ω_3, induced in a second-order process by the excitation waves at frequencies ω_1 and ω_2 is given by a product:

$$\boldsymbol{P}_{\mathrm{s}}^{(2)}(\boldsymbol{r},\omega_3) = \varepsilon_0 \delta(\boldsymbol{r}-\boldsymbol{r}_{\mathrm{s}})\, \underline{\underline{\chi}}_{\mathrm{s}}^{(2)}(\omega_1,\omega_2,\omega_3) : \boldsymbol{E}(\boldsymbol{r},\omega_1)\boldsymbol{E}(\boldsymbol{r},\omega_2), \tag{2.21}$$

where δ is a Dirac delta function and $\boldsymbol{r}_{\mathrm{S}}$ is the position vector of the surface. From symmetry considerations, the second-order susceptibility tensor at the interface between isotropic and centrosymmetric materials has only three independent elements: $\chi^{(2)}_{\perp\perp\perp}$, $\chi^{(2)}_{\perp\parallel\parallel}$ and $\chi^{(2)}_{\parallel\parallel\perp}$,[23] where $\perp$ and $\parallel$ denote perpendicular and parallel to the surface components, respectively. Thus, the surface non-linear polarization for a second-order process can be written in a simplified form (here, we also omit spatial dependence of the fields):

$$\boldsymbol{P}_{\mathrm{s}}^{(2)} = \varepsilon_0 \left[\boldsymbol{u}_{\perp} \left(\chi^{(2)}_{\perp\perp\perp} E_{\perp}^{\omega_1} E_{\perp}^{\omega_2} + \chi^{(2)}_{\perp\parallel\parallel} E_{\parallel}^{\omega_1} E_{\parallel}^{\omega_2} \right) + \boldsymbol{u}_{\parallel} \chi^{(2)}_{\parallel\perp\parallel} \left(E_{\perp}^{\omega_1} E_{\parallel}^{\omega_2} + E_{\parallel}^{\omega_1} E_{\perp}^{\omega_2} \right) \right], \tag{2.22}$$

where $\boldsymbol{u}_\perp$ and $\boldsymbol{u}_\parallel$ denote respectively unit vectors orthogonal and parallel to the surface. It should be noted, however, that surfaces of crystalline materials, even simple crystal classes, such as cubic, exhibit additional independent $\underline{\underline{\chi}}_{\mathrm{s}}^{(2)}$ elements (making up a total of 11 non-vanishing elements), which are anisotropic, *i.e.* which are dependent on the angle between pump polarization and crystalline axes.[41,42]

According to Rudnick and Stern,[43] the three tensor elements can be related to the frequency-dependent linear electric permittivity $\varepsilon(\omega)$ of the metal *via* the phenomenological parameters *a* and *b*:

$$\chi_{\perp\perp\perp}^{(2)} = a(\omega)\frac{e\varepsilon_0}{8m\omega^2}(\varepsilon(\omega)-1) \tag{2.23}$$

$$\chi_{\parallel\parallel\perp}^{(2)} = b(\omega)\frac{e\varepsilon_0}{8m\omega^2}(\varepsilon(\omega)-1) \tag{2.24}$$

where *e* and *m* denote the electron charge and mass. The third element, $\chi_{\perp\parallel\parallel}^{(2)}$, was shown to be negligible.[44,45] Besides, Rudnick and Stern distinguish another component of the second-order susceptibility that is related to the bulk contribution, $\chi_{\mathrm{bulk}}^{(2)} = d(\omega)\frac{e\varepsilon_0}{8m\omega^2}(\varepsilon(\omega)-1)$, and will be discussed in the following section.

Typically, in the case of an interface between an isotropic metal and an isotropic dielectric, eqn (2.22) can be simplified even further:

$$P_{\mathrm{s}\perp}^{(2)} = \varepsilon_0\chi_{\perp\perp\perp}^{(2)}|E_\perp|^2, \tag{2.25}$$

while the in-plane component of the non-linear surface polarization can be neglected, $P_{\mathrm{s}\parallel}^{(2)} = 0$, since $\chi_{\perp\perp\perp}^{(2)}$ is larger than other surface and bulk contributions by at least an order of magnitude.[44,46–49] Experimentally obtained absolute values of $\chi_{\perp\perp\perp}^{(2)}$ in SHG experiments with the excitation wavelength $\lambda_0 = 810$ nm, widely used for plasmonic metals, are 7.67×10^{-20} m^2 for gold, 1.07×10^{-19} $\mathrm{m}^2\,\mathrm{V}^{-1}$ for silver, 5.00×10^{-20} $\mathrm{m}^2\,\mathrm{V}^{-1}$ for copper and 1.00×10^{-18} $\mathrm{m}^2\,\mathrm{V}^{-1}$ for aluminum.[48]

When the simplified eqn (2.25) is combined with an appropriate numerical technique, for example, based on the boundary elements method, this simplification allows us to efficiently and accurately model surface SHG from metallic nanostructures.[50–53] Here, we consider the topical example of a gold nanoparticle immersed in water, *i.e.* the background permittivity is $\varepsilon_{\mathrm{m}} = 1.77$, that mimics typical experimental conditions,[54] simulated using the surface integral equation (SIE) approach.[55] Figure 2.6 shows the linear surface charge density and the non-linear polarization distributions at the surface of a spherical nanoparticle that has a diameter of 40 nm, as well as the linear and non-linear near- and far-field distributions, when it is excited at the fundamental wavelength $\lambda_0 = 800$ nm. Whereas the linear response of the nanoparticle is purely dipolar, the second-harmonic radiation shows

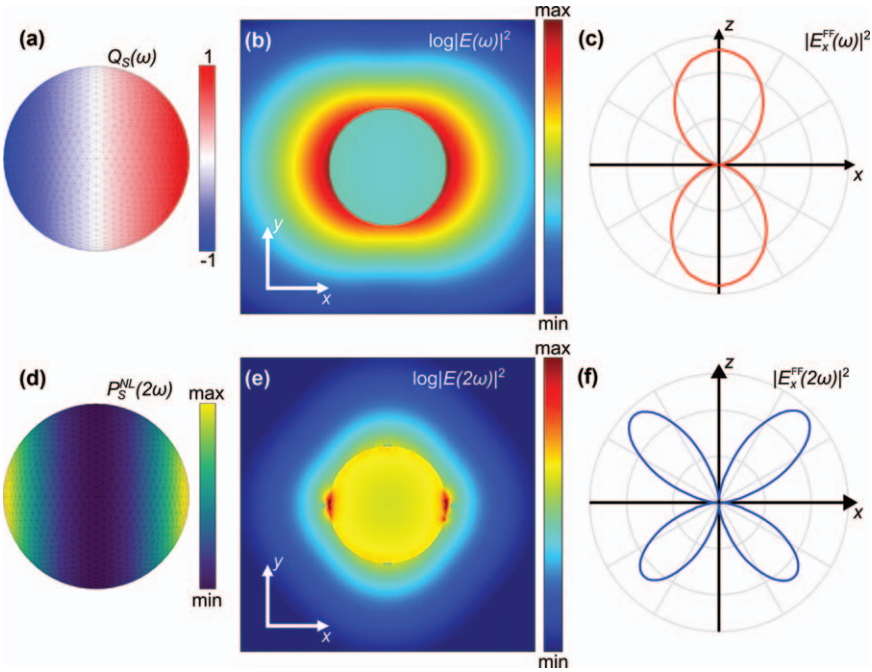

Figure 2.6 Linear and second-harmonic response of gold nanoparticle immersed in water [refractive index $(n) = 1.33$] with diameter of 50 nm under plane-wave excitation. (a) Normalized electric charge density distribution at the surface of the sphere. (b) Pseudo-color image of the scattered electric field in the linear regime (logarithmic scale). (c) Far-field distribution of the *x*-component of the scattered electric field (normalized). (d) Non-linear polarization distribution at the surface of the sphere. (e) Pseudo-color image of the electric field at the second-harmonic frequency (logarithmic scale). (f) *x*-Component of the SHG radiation pattern (normalized).

distinct quadrupolar features. This can be clearly seen from the angular distribution of the *x*-polarized component of the SHG, shown in Figure 2.6(f), which exhibits four petals in the scattering diagram that is typical feature of quadrupolar emission. This observation is consistent with a mode analysis based on the non-linear Mie theory[53,56–60] as well as some other analytical models.[61–63]

2.5 Bulk Non-linear Effects

In this section we review second- and third-order non-linear effects that stem from the bulk structure of the material. Among the second order processes, we highlight SHG in both symmetric and non-centrosymmetric media. For the third-order processes, we briefly review some parametric and nonparametric processes that occur in various materials.

2.5.1 Second-order Non-linearities

As opposed to surface non-linearities, only non-centrosymmetric systems and materials exhibit a bulk second-order non-linear response. Thus, the number of independent non-zero elements for the second-order susceptibility tensor $\underline{\chi}_{\mathrm{s}}^{(2)}$ depends on the microscopic symmetries of the material. The second-order bulk polarization is given by:

$$P_{\mathrm{b}}^{(2)}(\boldsymbol{r},\omega_3) = \varepsilon_0 \boldsymbol{\chi}_{\mathrm{b}}^{(2)}(\omega_1,\omega_2,\omega_3) : \boldsymbol{E}(\boldsymbol{r},\omega_1)\boldsymbol{E}(\boldsymbol{r},\omega_2). \tag{2.26}$$

Plugging this non-linear polarization into the wave equation [eqn (2.5)] allows finding nanostructure geometries that produce significant enhancement of SHG (as well as other second-order non-linear processes) in the presence of resonances at the fundamental and/or second-harmonic (or other involved waves) frequencies.[11] In practice, however, fabrication of such resonant nanostructures is complicated due to the difficulty of nanoscale patterning of non-linear materials. Only in recent years have progress in the nanoprocessing techniques for noncentrosymmetric group III–V compound semiconductors, such as GaAs,[64,65] GaP[66–68] and AlGaAs,[69–73] and advances in thin-film $LiNbO_3$ technology, allowed the experimental realization of such nanostructures.[74] We shall return to the discussion of enhancement of the non-linear response in the nanostructured non-centrosymmetric materials in Section 2.6.

Although in centrosymmetric material systems, the second-order non-linear response predominantly stems from the effective surface contribution, the bulk contribution to non-linear response cannot be neglected in certain configurations when the dipole approximation is no longer applicable, in particular when strong electric field gradients are present.[63,75,76] In this case, the non-linear bulk polarization can be rewritten to include quadrupolar terms:[76]

$$\boldsymbol{P}_{\mathrm{b}}^{(2)} = \varepsilon_0(\beta \boldsymbol{E}\nabla\cdot\boldsymbol{E} + \gamma\nabla(\boldsymbol{E}\cdot\boldsymbol{E}) + \delta'(\boldsymbol{E}\cdot\nabla)\boldsymbol{E}), \tag{2.27}$$

where β, γ and δ' are the material parameters that describe the electric quadrupole and magnetic dipole interactions. This bulk contribution is also often referred to as nonlocal,[45] since it involves the spatial derivatives of the electric fields, making the non-linear polarization at a point $\boldsymbol{r}$ in space dependent on the electric field at other points $\boldsymbol{r}'$. Although bulk and surface contributions to SHG from noble metal surfaces were shown to be distinguishable,[44] the bulk contribution is often considered to be negligible. Furthermore, since noble metals are opaque to electromagnetic radiation at optical frequencies, the non-linear phenomena occur in the vicinity of the surface, within the penetration depth (a few tens of nanometers), being effectively a surface effect. On the other hand, bulk contributions were shown to have a significant role in the second-order non-linear processes in centrosymmetric dielectrics, such as Si[77–80] and Ge.[81]

2.5.2 Third-order Non-linearities

Since third-order non-linear effects also exist in the presence of an inversion symmetry in the system, third-order (and higher odd-order) susceptibilities are non-zero in the bulk of a much wider range of materials, regardless of their structural symmetries and state.[8,13] For example, THG generation was demonstrated in both crystalline and amorphous solids,[82] in liquids,[83] gases,[84] and even in plasma.[85] Microscopic symmetries of the materials define the number of non-zero and independent elements of the $\underset{\equiv}{\chi}^{(3)}$ tensor.[13]

Let us consider here an illustrative example of a dielectric that has a simple cubic crystal structure. Under plane wave excitation along the z-axis (in a Cartesian coordinate system), only two elements of the $\underset{\equiv}{\chi}^{(3)}$ tensor contribute to the THG process:[8,41,86] $\chi^{(3)}_{xxyy}$ and $\chi^{(3)}_{xxxx}$. Thus, the components of the third order non-linear polarization in a THG process are given by the following expression:

$$P_j^{3\omega} = \varepsilon_0 \left(3\chi^{(3)}_{xxyy} E_j (\boldsymbol{E}\cdot\boldsymbol{E}) + \left(\chi^{(3)}_{xxxx} - 3\chi^{(3)}_{xxyy} \right) {E_j}^3 \right), \tag{2.28}$$

where index $j = x, y, z$ denotes the Cartesian component of the induced polarization.

In the case of an isotropic medium $\left(\chi^{(3)}_{xxxx} = 3\chi^{(3)}_{xxyy} = \chi^{(3)}_{\|\|\|\|} \right)$, eqn (2.28) is reduced even further since the third-harmonic polarization is parallel to the excitation electric field:

$$P_{\|}^{3\omega} = \varepsilon_0 \chi^{(3)}_{\|\|\|\|} (E_{\|})^3. \tag{2.29}$$

It should be noted that metals with a cubic crystal structure (such as the plasmonic metals mentioned in the previous section) also exhibit THG upon illumination with intense optical fields, however it can be mostly observed in reflection,[87,88] since metals are essentially opaque at optical frequencies, which renders the description of this process considerably more involved.[86]

The intensity-dependent refractive index, also referred to as the optical Kerr effect, briefly mentioned in Section 2.3, is another parametric third-order non-linear phenomenon, which is widely utilized in various optical devices. For example, the Kerr effect gives rise to various self-action processes, such as self-focusing,[89] and self-trapping,[90] and enables optical biostability for all-optical switching,[91] as well as soliton propagation of laser pulses.[13] In its simplest form, the non-linear index of refraction is given by the expression:

$$n = n_1 + n_2 I \tag{2.30}$$

where n_1 denotes the (usual) linear refractive index of the medium and n_2 is the second-order refractive index and I is the time-averaged intensity of the electric field, given by $I = 2{n'}_1 \varepsilon_0 c |\boldsymbol{E}|^2$. It can be shown that the non-linear refractive index is related to the susceptibility by:

$$n = \sqrt{1 + \chi^{(1)} + 3\chi^{(3)} |\boldsymbol{E}|^2}. \tag{2.31}$$

where we omit the indices of the susceptibility tensors, assuming an isotropic non-linear medium.

Apart from the parametric four-wave processes, such as THG and Kerr effect discussed above, other third-order processes, such as two photon absorption (TPA), saturable absorption[92] and stimulated Raman scattering,[93,94] have been studied in a vast variety of samples.[13] These nonparametric processes involve a net energy (or momentum) exchange between the optical field and the material, *i.e.* the electromagnetic wave exerts work on the medium. In a quantum-mechanical picture, upon interaction with light, matter undergoes a transition from one real quantum state to another one, as opposed to a parametric process, where the final matter state remains unchanged and involves only short transitions to virtual levels. In the case of TPA, two photons are simultaneously (*via* a virtual level) absorbed to excite an atom of the non-linear medium to a real state. Within our formalism, such nonparametric processes can be described using a complex susceptibility:

$$\underline{\underline{\chi}}^{(3)} = \underline{\underline{\chi}}'^{(3)} + j\underline{\underline{\chi}}''^{(3)}, \tag{2.32}$$

where $\underline{\underline{\chi}}'^{(3)}$ and $\underline{\underline{\chi}}''^{(3)}$ denote the real and imaginary parts of the third-order susceptibility, respectively.

Among the materials discussed above, gold possesses a large, complex, third-order susceptibility[95] that manifests in both THG[87,96,97] and TPA,[98,99] and has been interrogated using various experimental techniques, *e.g.* z-scan[100] and non-linear photoluminescence (also often referred to as two-photon photoluminescence) microscopy and spectroscopy. The exact mechanism of TPA in plasmonic metals remains under debate, especially in nanostructures, where it can be altered by the excitation of the resonances.[101–106] One of the widely accepted plausible explanations is that TPA is an effective third-order process, which involves two subsequent linear photon absorptions *via* a real intermediate state, *i.e.* it is a cascaded $\underline{\chi} : \underline{\chi}$ absorption related to the linear susceptibility,[107] rather than a coherent TPA. More recently, new models of non-linear absorption and photoluminescence have been discussed, which, in particular, highlight the role of quantum[108] and electronic thermal effects.[109–111]

Non-linear absorption is closely related to the topic of optical breakdown – irreversible material damage caused by strong interaction of matter with intense laser pulses.[11] Multiphoton ionization of atoms can occur upon excitation with a laser beam that has an intensity on the order of 10^{-11} W^{-2}. Although destructive effects caused by the optical breakdown are often undesirable, a controlled disruption or modification (such as two-photon polymerization[112]) of the materials is widely applied in modern laser-based nanoprocessing technologies. Here, we mention a few notable examples, not attempting to provide an exhaustive list: 3D microscale and nanoscale printing using photosensitive polymers,[113–115] plasmonic color printing using pulsed laser-writing,[116–118] ablation of nanoparticles,[119–121] and

pulsed laser deposition,[122–124] whereas many other examples of detailed descriptions of these nanofabrication methods are provided later in this book.

2.6 Enhancement of Non-linear Effects with Nanostructures

The standard approach for maximizing the non-linear conversion efficiency in traditional non-linear optics – the phase matching technique – is often not applicable in nanostructures, since their characteristic dimensions are smaller than the operational wavelength. Thus, alternative methods are desired to enhance both surface and bulk non-linear phenomena in nanostructured materials, which we briefly overview in this section.

As mentioned in Section 2.4, surface non-linear effects are typically weak due to a low light–matter interaction volume, however, they can be enhanced by virtue of field enhancement associated with the excitation of SP resonance, even in the simplest prism-coupling (also known as Kretschmann) configuration.[36] Bulk non-linearities in dielectrics can be enhanced in a similar way, by interfacing a non-linear dielectric with a plasmonic metal.[125] Figure 2.7(a) shows schematics for an experimental demonstration of SPP-mediated SHG in a non-linear (non-centrosymmetric) crystal placed atop of a thin gold film.[126] Such a simple arrangement can be improved by nanopatterning the metal film in the lateral dimensions to match a specific resonance wavelength and produce a stronger field enhancement to amplify the targeted non-linear process.[127–139]

A particularly versatile and robust way to achieve such a resonant enhancement relies on rationally designed plasmonic metasurfaces – arrays of plasmonic resonators with subwavelength dimensions and period –, which, in recent years, became the subject of a broad interest in the research community.[140–145] One of the first experimental demonstrations is shown in Figure 2.7(b), where the resonant plasmonic metasurfaces are coupled to the resonance of the underlying non-linear material, which allowed achievement of three orders of magnitude SHG enhancement.[146] Yet, SHG can be amplified even further by nanostructuring also the non-linear dielectric itself, such that it supports even stronger field enhancement. Figure 2.7(c) shows an example of such a metasurface that comprises gold nanorings filled with $LiNbO_3$.[147]

More recently, group III–V compound semiconductors and $LiNbO_3$ metasurfaces became a subject of extensive research, enabled by the development of thin-film growth and its subsequent nanopatterning technologies. Such high-quality fabrication of dielectric nanostructures allows achievement of very high SHG yield in all-dielectric nanostructures,[148–151] without the need to resort to a plasmonic field enhancement. Figure 2.8(a) and (b) show two examples of such metasurfaces with record high SHG efficiencies, which were achieved using Mie-like[152] and Fano[153] resonances in thin-film

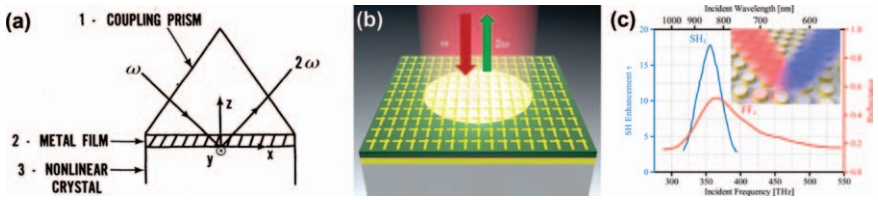

Figure 2.7 Various schemes for plasmonic enhancement of bulk SHG in non-linear dielectrics. (a) Kretschmann (prism-coupling) configuration for SPP-enhanced SHG in a bulk non-linear crystal. Reproduced from ref. 126 with permission from American Physical Society, Copyright 1984. (b) Resonant plasmonic metasurface-enhanced SHG. Reproduced from ref. 146 with permission from Springer Nature, Copyright 2014. (c) Non-linear dielectric-filled plasmonic ring resonators. Reproduced from ref. 147 with permission from American Chemical Society, Copyright 2015.

$LiNbO_3$ metasurfaces. Similar progress was reported for the third-order [Figure 2.8(c) and (d) show examples of enhanced THG in Si[154] and silicon nitride (SiN_x)[155] nanostructures] and even higher-order non-linear optical processes.[156–158]

Last, but not least, we should mention that the aforementioned benefits of nanostructured non-linear materials are also employed in the field of integrated optics. Non-linear components of integrated optical circuits are pivotal elements of optical signal processing devices, for instance, fast modulators, sum and difference frequency generators, isolators, and circulators, to name a few.[159] Although the phase-matching technique is applicable and widely used in optical waveguides, striving for miniaturization of photonic chips calls for alternative solutions that involve nanostructured materials. Figure 2.9 showcases two examples of waveguided SHG enhanced in a nanoscale form-factor. In both cases, devices are comprised of materials that are widely employed in standard photonic waveguide technologies: Figure 2.9(a) illustrates a $LiNbO_3$-based device,[160] where enhancement is achieved using metasurface-assisted phase matching, whereas Figure 2.9(b) shows a hybrid plasmonic–AlGaInP[161] waveguide, which benefits from the SPP field-enhancement.

2.7 Summary and Outlook

The different non-linear effects that can occur in materials have been discussed and illustrated with some recent examples from the scientific literature. We have attempted to keep the underlying formalism as simple as possible, avoiding for example a tensorial description throughout. However, the different examples that were discussed have also highlighted that this field of research is strongly linked to solid state physics and most effects depend on the anisotropy of the system under study. Whilst this renders non-linear optics complicated, it is also makes it fascinating and opens up

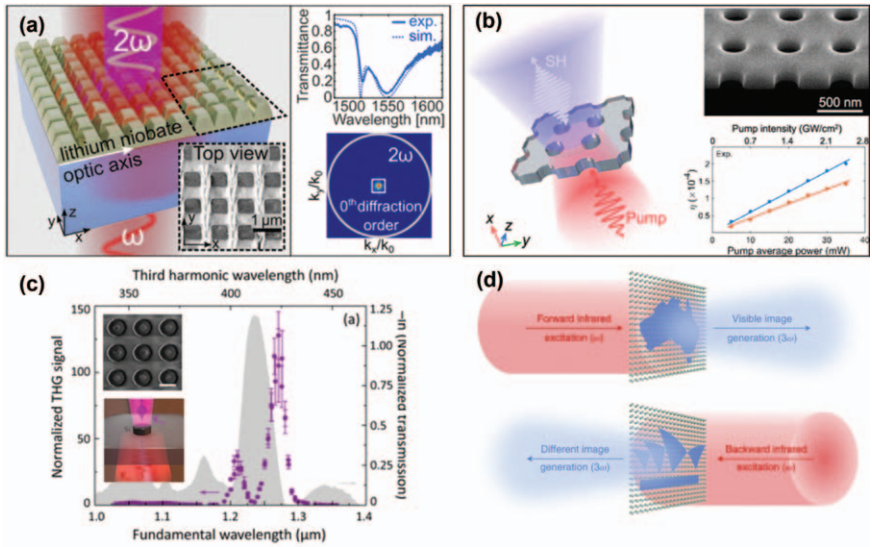

Figure 2.8 Enhancement of bulk non-linearities using resonances in dielectric nanostructures: (a) SHG in a resonant $LiNBO_3$ metasurface. Reproduced from ref. 152, with permission from American Chemical Society, Copyright 2020. (b) $LiNBO_3$ membrane-based non-linear metasurface. Reproduced from ref. 153 with permission from American Chemical Society, Copyright 2022. (c) THG in silicon nanoparticles. Reproduced from ref. 154 with permission from American Chemical Society, Copyright 2014. (d) Asymmetric THG image generation in Si/SiN_x-based metasurface. Reproduced from ref. 155 with permission from Springer Nature, Copyright 2022.

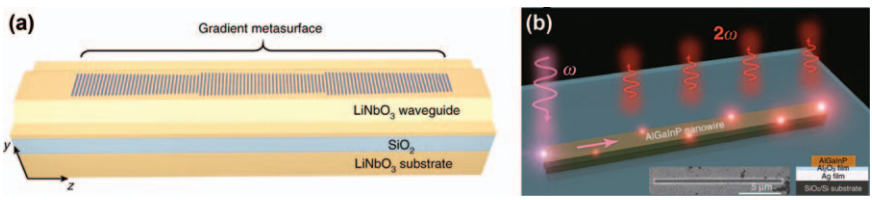

Figure 2.9 Examples in integrated optics. (a) Non-linear metasurface-enabled SHG in $LiNBO_3$ waveguide. Reproduced from ref. 160, https://doi.org/10.1038/s41467-017-02189-6, under the terms of the CC BY 4.0 license, https://creativecommons.org/licenses/by/4.0/. (b) SHG in a hybrid non-linear plasmonic waveguide. Reproduced from ref. 161, https://doi.org/10.1038/s41377-020-00414-4, under the terms of the CC BY 4.0 license, https://creativecommons.org/licenses/by/4.0/.

many different venues to exploit, tailor and control the non-linear response of materials and nanostructures. The strong optical fields required to trigger these non-linear effects can often produce catastrophic optical damage or

useful material modification, which are exploited in other chapters of this book.

Future fundamental research in this field of study should certainly focus on improving our understanding of the non-linear response of materials, including all its subtleties. These include the tensorial nature of the non-linear susceptibilities, and the distinguishability, competition, and/or correlation between surface and bulk non-linear effects. Overall, one may wish for a more quantitative description of the non-linear susceptibilities for a broad range of relevant materials, including for inhomogeneous systems that can include several phases. Such data are the prerequisite for more accurate numerical models of light–matter interactions in the non-linear regime.[55,58]

References

1. D. Falk, D. Brill and D. Stork, *Seeing the light*, Wiley, Hoboken, 1986.
2. H. E. Edens, *Appl. Opt.*, 2015, **54**, B26–B34.
3. C. F. Bohren and D. R. Huffman, *Absorption and Scattering of Light by Small Particles*, Wiley Interscience, 1983.
4. J. D. Jackson, *Classical Electrodynamics*, Wiley, New York, 3rd edn, 1999.
5. G. B. Arfken and H. J. Weber, *Mathematical Methods for Physicists*, Elsevier Academic Press, 6th edn, 2005.
6. R. A. Johnson, *Phys. Rev. B: Condens. Matter Mater. Phys.*, 1988, **37**, 3924–3931.
7. G. A. Jones and D. S. Bradshaw, *Front. Phys.*, 2019, **7**, 100.
8. J. A. Armstrong, N. Bloembergen, J. Ducuing and P. S. Pershan, *Phys. Rev.*, 1962, **127**, 1918–1939.
9. J. Van Kranendonk and J. E. Sipe, in *Progress in Optics*, ed. E. Wolf, Elsevier, 1977, vol. 15, pp. 245–350.
10. P. E. Powers and H. A. Haus, *Fundamentals of nonlinear optics*, Taylor and Francis, Boca Raton, 2nd edn, 2017.
11. Y. R. Shen, *The Principles of Nonlinear Optics*, Wiley, Hoboken, 1984.
12. B. E. A. Saleh and M. C. Teich, *Fundamental of photonics*, Wiley, Hoboken, 3rd edn, 2019.
13. R. W. Boyd, *Nonlinear Optics*, Elsevier Science, London, 4th edn, 2020.
14. O. J. F. Martin, A. Dereux and C. Girard, *J. Opt. Soc. Am. A*, 1994, **11**, 1073–1080.
15. W. J. Nie, *Adv. Mater.*, 1993, **5**, 520–545.
16. Q. L. Meng, Z. L. Su, J. L. Yu and B. Zhang, *Conference on Optomechanical Engineering*, San Diego, CA, 2015.
17. J. R. Lakowicz, *Principles of Fluorescence Spectroscopy*, Kluwer Academic/Plenum, New York, 2nd edn, 1999.
18. J. Butet and O. J. F. Martin, *J. Nanophotonics*, 2017, **11**, 16007.
19. S. Kharratian, H. Urey and M. C. Onbasli, *Adv. Opt. Mater.*, 2020, **8**, 1901381.
20. T. Y. F. Tsang, *Phys. Rev. A: At., Mol., Opt. Phys.*, 1995, **52**, 4116–4125.

21. P. N. Saeta and N. A. Miller, *Appl. Phys. Lett.*, 2001, **79**, 2704–2706.
22. N. Bloembergen, *Appl. Phys. B: Lasers Opt.*, 1999, **68**, 289–293.
23. P. Guyot-Sionnest, W. Chen and Y. R. Shen, *Phys. Rev. B: Condens. Matter Mater. Phys.*, 1986, **33**, 8254–8263.
24. Y. R. Shen, *Annu. Rev. Phys. Chem.*, 1989, **40**, 327–350.
25. Y. R. Shen, *J. Opt. Soc. Am. B*, 2011, **28**, A56–A66.
26. R. W. Terhune, P. D. Maker and C. M. Savage, *Phys. Rev. Lett.*, 1962, **8**, 404–406.
27. F. Brown, R. E. Parks and A. M. Sleeper, *Phys. Rev. Lett.*, 1965, **14**, 1029–1031.
28. N. Bloembergen, R. K. Chang, S. S. Jha and C. H. Lee, *Phys. Rev.*, 1968, **174**, 813–822.
29. M. Kauranen and A. V. Zayats, *Nat. Photonics*, 2012, **6**, 737–748.
30. D. K. Gramotnev and S. I. Bozhevolnyi, *Nat. Photonics*, 2010, **4**, 83–91.
31. G. S. Agarwal and S. S. Jha, *Solid State Commun.*, 1982, **41**, 499–501.
32. S. A. Maier, *Plasmonics: Fundamentals and Applications*, Springer, 2007.
33. G.-C. Li, D. Lei, M. Qiu, W. Jin, S. Lan and A. V. Zayats, *Nat. Commun.*, 2021, **12**, 4326.
34. H. Raether, *Surface Plasmons on Smooth and Rough Surfaces and on Gratings*, Springer, 1988.
35. J. P. Kottmann, O. J. F. Martin, D. R. Smith and S. Schultz, *Chem. Phys. Lett.*, 2001, **341**, 1–6.
36. H. J. Simon, D. E. Mitchell and J. G. Watson, *Phys. Rev. Lett.*, 1974, **33**, 1531–1534.
37. J. Butet, P.-F. Brevet and O. J. F. Martin, *ACS Nano*, 2015, **9**, 10545–10562.
38. N. C. Panoiu, W. E. I. Sha, D. Y. Lei and G. C. Li, *J. Opt.*, 2018, **20**, 083001.
39. P. Dombi, Z. Pápa, J. Vogelsang, S. V. Yalunin, M. Sivis, G. Herink, S. Schäfer, P. Groß, C. Ropers and C. Lienau, *Rev. Mod. Phys.*, 2020, **92**, 025003.
40. T. Pertsch and Y. Kivshar, *MRS Bull.*, 2020, **45**, 210–220.
41. J. E. Sipe, D. J. Moss and H. M. van Driel, *Phys. Rev. B: Condens. Matter Mater. Phys.*, 1987, **35**, 1129–1141.
42. S. Boroviks, T. Yezekyan, A. R. Echarri, F. J. G. de Abajo, J. D. Cox, S. I. Bozhevolnyi, N. A. Mortensen and C. Wolff, *Opt. Lett.*, 2021, **46**, 833–836.
43. J. Rudnick and E. A. Stern, *Phys. Rev. B: Condens. Matter Mater. Phys.*, 1971, **4**, 4274–4290.
44. F. X. Wang, F. J. Rodríguez, W. M. Albers, R. Ahorinta, J. E. Sipe and M. Kauranen, *Phys. Rev. B: Condens. Matter Mater. Phys.*, 2009, **80**, 233402.
45. G. Bachelier, J. Butet, I. Russier-Antoine, C. Jonin, E. Benichou and P. F. Brevet, *Phys. Rev. B: Condens. Matter Mater. Phys.*, 2010, **82**, 235403.
46. S. S. Jha, *Phys. Rev. Lett.*, 1965, **15**, 412–414.
47. S. S. Jha, *Phys. Rev.*, 1965, **140**, A2020–A2030.
48. D. Krause, C. W. Teplin and C. T. Rogers, *J. Appl. Phys.*, 2004, **96**, 3626–3634.

49. G. Bachelier, J. Butet, I. Russier-Antoine, C. Jonin, E. Benichou and P.-F. Brevet, *Phys. Rev. B: Condens. Matter Mater. Phys.*, 2010, **82**, 235403.
50. J. Butet, G. Bachelier, I. Russier-Antoine, C. Jonin, E. Benichou and P. F. Brevet, *Phys. Rev. Lett.*, 2010, **105**, 077401.
51. J. Mäkitalo, S. Suuriniemi and M. Kauranen, *Opt. Express*, 2011, **19**, 23386–23399.
52. C. Forestiere, A. Capretti and G. Miano, *J. Opt. Soc. Am. B*, 2013, **30**, 2355–2364.
53. J. Butet, G. D. Bernasconi, M. Petit, A. Bouhelier, C. Yan, O. J. F. Martin, B. Cluzel and O. Demichel, *ACS Photonics*, 2017, **4**, 2923–2929.
54. J. Butet, J. Duboisset, G. Bachelier, I. Russier-Antoine, E. Benichou, C. Jonin and P.-F. Brevet, *Nano Lett.*, 2010, **10**, 1717–1721.
55. J. Butet, B. Gallinet, K. Thyagarajan and O. J. F. Martin, *J. Opt. Soc. Am. B*, 2013, **30**, 2970–2979.
56. I. Russier-Antoine, E. Benichou, G. Bachelier, C. Jonin and P.-F. Brevet, *J. Phys. Chem. C*, 2007, **111**, 9044–9048.
57. J. Butet, I. Russier-Antoine, C. Jonin, N. Lascoux, E. Benichou and P.-F. Brevet, *J. Opt. Soc. Am. B*, 2012, **29**, 2213–2221.
58. J. Butet, S. Dutta-Gupta and O. J. F. Martin, *Phys. Rev. B: Condens. Matter Mater. Phys.*, 2014, **89**, 245449.
59. G. D. Bernasconi, J. Butet and O. J. F. Martin, *J. Opt. Soc. Am. B*, 2016, **33**, 768–779.
60. J. Butet, A. Maurice, E. Bergmann, G. Bachelier, I. Russier-Antoine, C. Ray, O. Bonhomme, C. Jonin, E. Benichou and P.-F. Brevet, in *Metal Nanostructures for Photonics*, ed. L. R. P. Kassab and C. B. de Araujo, Elsevier, 2019, pp. 105–131.
61. J. I. Dadap, J. Shan, K. B. Eisenthal and T. F. Heinz, *Phys. Rev. Lett.*, 1999, **83**, 4045–4048.
62. J. I. Dadap, J. Shan and T. F. Heinz, *J. Opt. Soc. Am. B*, 2004, **21**, 1328–1347.
63. C. Ciracì, E. Poutrina, M. Scalora and D. R. Smith, *Phys. Rev. B: Condens. Matter Mater. Phys.*, 2012, **86**, 115451.
64. S. Liu, M. B. Sinclair, S. Saravi, G. A. Keeler, Y. Yang, J. Reno, G. M. Peake, F. Setzpfandt, I. Staude, T. Pertsch and I. Brener, *Nano Lett.*, 2016, **16**, 5426–5432.
65. F. J. F. Löchner, A. N. Fedotova, S. Liu, G. A. Keeler, G. M. Peake, S. Saravi, M. R. Shcherbakov, S. Burger, A. A. Fedyanin, I. Brener, T. Pertsch, F. Setzpfandt and I. Staude, *ACS Photonics*, 2018, **5**, 1786–1793.
66. J. Cambiasso, G. Grinblat, Y. Li, A. Rakovich, E. Cortés and S. A. Maier, *Nano Lett.*, 2017, **17**, 1219–1225.
67. A. P. Anthur, H. Zhang, R. Paniagua-Dominguez, D. A. Kalashnikov, S. T. Ha, T. W. W. Maß, A. I. Kuznetsov and L. Krivitsky, *Nano Lett.*, 2020, **20**, 8745–8751.
68. D. Khmelevskaia, D. I. Markina, V. V. Fedorov, G. A. Ermolaev, A. V. Arsenin, V. S. Volkov, A. S. Goltaev, Y. M. Zadiranov, I. A. Tzibizov, A. P.

Pushkarev, A. K. Samusev, A. A. Shcherbakov, P. A. Belov, I. S. Mukhin and S. V. Makarov, *Appl. Phys. Lett.*, 2021, **118**, 201101.
69. V. F. Gili, L. Carletti, A. Locatelli, D. Rocco, M. Finazzi, L. Ghirardini, I. Favero, C. Gomez, A. Lemaître, M. Celebrano, C. De Angelis and G. Leo, *Opt. Express*, 2016, **24**, 15965–15971.
70. L. Ghirardini, L. Carletti, V. Gili, G. Pellegrini, L. Duò, M. Finazzi, D. Rocco, A. Locatelli, C. De Angelis, I. Favero, M. Ravaro, G. Leo, A. Lemaître and M. Celebrano, *Opt. Lett.*, 2017, **42**, 559–562.
71. L. Carletti, D. Rocco, A. Locatelli, C. De Angelis, V. F. Gili, M. Ravaro, I. Favero, G. Leo, M. Finazzi, L. Ghirardini, M. Celebrano, G. Marino and A. V. Zayats, *Nanotechnology*, 2017, **28**, 114005.
72. P. P. Vabishchevich, S. Liu, M. B. Sinclair, G. A. Keeler, G. M. Peake and I. Brener, *ACS Photonics*, 2018, **5**, 1685–1690.
73. K. Koshelev, S. Kruk, E. Melik-Gaykazyan, J.-H. Choi, A. Bogdanov, H.-G. Park and Y. Kivshar, *Science*, 2020, **367**, 288–292.
74. M. Yamada, N. Nada, M. Saitoh and K. Watanabe, *Appl. Phys. Lett.*, 1993, **62**, 435–436.
75. P. Guyot-Sionnest and Y. R. Shen, *Phys. Rev. B: Condens. Matter Mater. Phys.*, 1987, **35**, 4420–4426.
76. P. Guyot-Sionnest and Y. R. Shen, *Phys. Rev. B: Condens. Matter Mater. Phys.*, 1988, **38**, 7985–7989.
77. D. E. Milovzorov, A. M. Ali, T. Inokuma, Y. Kurata, T. Suzuki and S. Hasegawa, *Thin Solid Films*, 2001, **382**, 47–55.
78. P. R. Wiecha, A. Arbouet, C. Girard, T. Baron and V. Paillard, *Phys. Rev. B: Condens. Matter Mater. Phys.*, 2016, **93**, 125421.
79. S. V. Makarov, M. I. Petrov, U. Zywietz, V. Milichko, D. Zuev, N. Lopanitsyna, A. Kuksin, I. Mukhin, G. Zograf, E. Ubyivovk, D. A. Smirnova, S. Starikov, B. N. Chichkov and Y. S. Kivshar, *Nano Lett.*, 2017, **17**, 3047–3053.
80. D. Timbrell, J. W. You, Y. S. Kivshar and N. C. Panoiu, *Sci. Rep.*, 2018, **8**, 3586.
81. Y. Wang, D. Burt, K. Lu and D. Nam, *Appl. Phys. Lett.*, 2022, **120**, 242105.
82. D. J. Moss, E. C. Fox, J. E. Sipe and H. M. van Driel, *International Conference on Quantum Electronics*, Tokyo, 1988.
83. F. Kajzar and J. Messier, *Phys. Rev. A: At., Mol., Opt. Phys.*, 1985, **32**, 2352–2363.
84. G. H. C. New and J. F. Ward, *Phys. Rev. Lett.*, 1967, **19**, 556–559.
85. J. L. Bobin, M. Decroisette, B. Meyer and Y. Vitel, *Phys. Rev. Lett.*, 1973, **30**, 594–597.
86. W. K. Burns and N. Bloembergen, *Phys. Rev. B: Condens. Matter Mater. Phys.*, 1971, **4**, 3437–3450.
87. N. Bloembergen, W. K. Burns and M. Matsuoka, *Opt. Commun.*, 1969, **1**, 195–198.
88. C. C. Wang and E. L. Baardsen, *Phys. Rev.*, 1969, **185**, 1079–1082.
89. P. L. Kelley, *Phys. Rev. Lett.*, 1965, **15**, 1005–1008.

90. R. Y. Chiao, E. Garmire and C. H. Townes, *Phys. Rev. Lett.*, 1964, **13**, 479–482.
91. A. Szöke, V. Daneu, J. Goldhar and N. A. Kurnit, *Appl. Phys. Lett.*, 2003, **15**, 376–379.
92. L. W. Tutt and T. F. Boggess, *Prog. Quantum Electron.*, 1993, **17**, 299–338.
93. R. R. Jones, D. C. Hooper, L. Zhang, D. Wolverson and V. K. Valev, *Nanoscale Res. Lett.*, 2019, **14**, 231.
94. J. Langer, D. Jimenez de Aberasturi, J. Aizpurua, R. A. Alvarez-Puebla, B. Auguié, J. J. Baumberg, G. C. Bazan, S. E. J. Bell, A. Boisen, A. G. Brolo, J. Choo, D. Cialla-May, V. Deckert, L. Fabris, K. Faulds, F. J. García de Abajo, R. Goodacre, D. Graham, A. J. Haes, C. L. Haynes, C. Huck, T. Itoh, M. Käll, J. Kneipp, N. A. Kotov, H. Kuang, E. C. Le Ru, H. K. Lee, J.-F. Li, X. Y. Ling, S. A. Maier, T. Mayerhöfer, M. Moskovits, K. Murakoshi, J.-M. Nam, S. Nie, Y. Ozaki, I. Pastoriza-Santos, J. Perez-Juste, J. Popp, A. Pucci, S. Reich, B. Ren, G. C. Schatz, T. Shegai, S. Schlücker, L.-L. Tay, K. G. Thomas, Z.-Q. Tian, R. P. Van Duyne, T. Vo-Dinh, Y. Wang, K. A. Willets, C. Xu, H. Xu, Y. Xu, Y. S. Yamamoto, B. Zhao and L. M. Liz-Marzán, *ACS Nano*, 2020, **14**, 28–117.
95. R. W. Boyd, Z. Shi and I. De Leon, *Opt. Commun.*, 2014, **326**, 74–79.
96. M. Lippitz, M. A. van Dijk and M. Orrit, *Nano Lett.*, 2005, **5**, 799–802.
97. J. Renger, R. Quidant, N. van Hulst and L. Novotny, *Phys. Rev. Lett.*, 2010, **104**, 046803.
98. E. Xenogiannopoulou, P. Aloukos, S. Couris, E. Kaminska, A. Piotrowska and E. Dynowska, *Opt. Commun.*, 2007, **275**, 217–222.
99. N. Rotenberg, A. D. Bristow, M. Pfeiffer, M. Betz and H. M. van Driel, *Phys. Rev. B: Condens. Matter Mater. Phys.*, 2007, **75**, 155426.
100. M. Sheik-Bahae, A. A. Said, T. H. Wei, D. J. Hagan and E. W. V. Stryland, *IEEE J. Quantum Electron.*, 1990, **26**, 760–769.
101. K. Imura, T. Nagahara and H. Okamoto, *J. Phys. Chem. B*, 2005, **109**, 13214–13220.
102. P. Biagioni, D. Brida, J.-S. Huang, J. Kern, L. Duò, B. Hecht, M. Finazzi and G. Cerullo, *Nano Lett.*, 2012, **12**, 2941–2947.
103. X.-F. Jiang, Y. Pan, C. Jiang, T. Zhao, P. Yuan, T. Venkatesan and Q.-H. Xu, *J. Phys. Chem. Lett.*, 2013, **4**, 1634–1638.
104. R. Méjard, A. Verdy, M. Petit, A. Bouhelier, B. Cluzel and O. Demichel, *ACS Photonics*, 2016, **3**, 1482–1488.
105. E. Sakat, I. Bargigia, M. Celebrano, A. Cattoni, S. Collin, D. Brida, M. Finazzi, C. D'Andrea and P. Biagioni, *ACS Photonics*, 2016, **3**, 1489–1493.
106. D. Xie, F. O. Laforge, I. Grigorenko and H. A. Rabitz, *J. Opt. Soc. Am. B*, 2019, **36**, 1931–1936.
107. M. R. Beversluis, A. Bouhelier and L. Novotny, *Phys. Rev. B: Condens. Matter Mater. Phys.*, 2003, **68**, 115433.
108. S. Grossmann, D. Friedrich, M. Karolak, R. Kullock, E. Krauss, M. Emmerling, G. Sangiovanni and B. Hecht, *Phys. Rev. Lett.*, 2019, **122**, 246802.

109. K. Malchow and A. Bouhelier, *J. Opt. Soc. Am. B*, 2021, **38**, 576–583.
110. Á. Rodríguez Echarri, F. Iyikanat, S. Boroviks, N. A. Mortensen, J. D. Cox and F. J. García de Abajo, *ACS Photonics*, 2023, **10**, 2918–2929.
111. Y. Sivan, I. W. Un, I. Kalyan, K.-Q. Lin, J. M. Lupton and S. Bange, *ACS Nano*, 2023, **17**, 11439–11453.
112. S. O'Halloran, A. Pandit, A. Heise and A. Kellett, *Adv. Sci.*, 2023, **10**, 2204072.
113. N. Anscombe, *Nat. Photonics*, 2010, **4**, 22–23.
114. F. Niesler and M. Hermatschweiler, *Laser Tech. J.*, 2015, **12**, 44–47.
115. A. Bagheri and J. Jin, *ACS Appl. Polym. Mater.*, 2019, **1**, 593–611.
116. A. Kristensen, J. K. W. Yang, S. I. Bozhevolnyi, S. Link, P. Nordlander, N. J. Halas and N. A. Mortensen, *Nat. Rev. Mater.*, 2016, **2**, 16088.
117. J.-M. Guay, A. Calà Lesina, G. Côté, M. Charron, D. Poitras, L. Ramunno, P. Berini and A. Weck, *Nat. Commun.*, 2017, **8**, 16095.
118. A. S. Roberts, S. M. Novikov, Y. Yang, Y. Chen, S. Boroviks, J. Beermann, N. A. Mortensen and S. I. Bozhevolnyi, *ACS Nano*, 2019, **13**, 71–77.
119. M. F. Becker, J. R. Brock, H. Cai, D. E. Henneke, J. W. Keto, J. Lee, W. T. Nichols and H. D. Glicksman, *Nanostruct. Mater.*, 1998, **10**, 853–863.
120. N. G. Semaltianos, *Crit. Rev. Solid State Mater. Sci.*, 2010, **35**, 105–124.
121. U. Zywietz, A. B. Evlyukhin, C. Reinhardt and B. N. Chichkov, *Nat. Commun.*, 2014, **5**, 3402.
122. C. T. Rogers, A. Inam, M. S. Hegde, B. Dutta, X. D. Wu and T. Venkatesan, *Appl. Phys. Lett.*, 1989, **55**, 2032–2034.
123. D. H. Lowndes, D. B. Geohegan, A. A. Puretzky, D. P. Norton and C. M. Rouleau, *Science*, 1996, **273**, 898–903.
124. N. A. Shepelin, Z. P. Tehrani, N. Ohannessian, C. W. Schneider, D. Pergolesi and T. Lippert, *Chem. Soc. Rev.*, 2023, **52**, 2294–2321.
125. H. J. Simon, R. E. Benner and J. G. Rako, *Opt. Commun.*, 1977, **23**, 245–248.
126. J. G. Rako, J. C. Quail and H. J. Simon, *Phys. Rev. B: Condens. Matter Mater. Phys.*, 1984, **30**, 5552–5559.
127. T. Y. F. Tsang, *Opt. Lett.*, 1996, **21**, 245–247.
128. W. Fan, S. Zhang, N. C. Panoiu, A. Abdenour, S. Krishna, R. M. Osgood, K. J. Malloy and S. R. J. Brueck, *Nano Lett.*, 2006, **6**, 1027–1030.
129. F. B. P. Niesler, N. Feth, S. Linden, J. Niegemann, J. Gieseler, K. Busch and M. Wegener, *Opt. Lett.*, 2009, **34**, 1997–1999.
130. P. Genevet, J.-P. Tetienne, E. Gatzogiannis, R. Blanchard, M. A. Kats, M. O. Scully and F. Capasso, *Nano Lett.*, 2010, **10**, 4880–4883.
131. E. Poutrina, C. Ciracì, D. J. Gauthier and D. R. Smith, *Opt. Express*, 2012, **20**, 11005–11013.
132. D. Bar-Lev and J. Scheuer, *Opt. Express*, 2013, **21**, 29165–29178.
133. I. De Leon, J. E. Sipe and R. W. Boyd, *Phys. Rev. A: At., Mol., Opt. Phys.*, 2014, **89**, 013855.
134. J. B. Lassiter, X. Chen, X. Liu, C. Ciracì, T. B. Hoang, S. Larouche, S.-H. Oh, M. H. Mikkelsen and D. R. Smith, *ACS Photonics*, 2014, **1**, 1212–1217.

135. C. Ciracì, M. Scalora and D. R. Smith, *Phys. Rev. B: Condens. Matter Mater. Phys.*, 2015, **91**, 205403.
136. M. Mesch, B. Metzger, M. Hentschel and H. Giessen, *Nano Lett.*, 2016, **16**, 3155–3159.
137. A. R. Echarri, J. D. Cox, R. Yu and F. J. García de Abajo, *ACS Photonics*, 2018, **5**, 1521–1527.
138. J. Gour, S. Beer, A. Alberucci, U. D. Zeitner and S. Nolte, *Opt. Lett.*, 2022, **47**, 6025–6028.
139. A. Chakraborty, P. Barman, A. K. Singh, X. Wu, D. A. Akimov, T. Meyer-Zedler, S. Nolte, C. Ronning, M. Schmitt, J. Popp and J.-S. Huang, *Laser Photonics Rev.*, 2023, **17**, 2200958.
140. M. Lapine, I. V. Shadrivov and Y. S. Kivshar, *Rev. Mod. Phys.*, 2014, **86**, 1093–1123.
141. K.-Y. Yang, R. Verre, J. Butet, C. Yan, T. J. Antosiewicz, M. Käll and O. J. F. Martin, *Nano Lett.*, 2017, **17**, 5258–5263.
142. E. Rahimi and R. Gordon, *Adv. Opt. Mater.*, 2018, **6**, 1800274.
143. A. Krasnok, M. Tymchenko and A. Alù, *Mater. Today*, 2018, **21**, 8–21.
144. M. J. Huttunen, R. Czaplicki and M. Kauranen, *J. Nonlinear Opt. Phys. Mater.*, 2019, **28**, 1950001.
145. P. Vabishchevich and Y. Kivshar, *Photonics Res.*, 2023, **11**, B50–B64.
146. J. Lee, M. Tymchenko, C. Argyropoulos, P.-Y. Chen, F. Lu, F. Demmerle, G. Boehm, M.-C. Amann, A. Alu and M. A. Belkin, *Nature*, 2014, **511**, 65–69.
147. D. Lehr, J. Reinhold, I. Thiele, H. Hartung, K. Dietrich, C. Menzel, T. Pertsch, E.-B. Kley and A. Tünnermann, *Nano Lett.*, 2015, **15**, 1025–1030.
148. D. Smirnova and Y. S. Kivshar, *Optica*, 2016, **3**, 1241–1255.
149. M. Rahmani, G. Leo, I. Brener, A. V. Zayats, S. A. Maier, C. D. Angelis, H. Tan, V. F. Gili, F. Karouta, R. Oulton, K. Vora, M. Lysevych, I. Staude, L. Xu, A. E. Miroshnichenko, C. Jagadish and D. N. Neshev, *Opto-Electron. Adv.*, 2018, **1**, 180021.
150. T. Liu, S. Xiao, B. Li, M. Gu, H. Luan and X. Fang, *Front. Nanotechnol.*, 2022, **4**, 891892.
151. D. Rocco, R. C. Morales, L. Xu, A. Zilli, V. Vinel, M. Finazzi, M. Celebrano, G. Leo, M. Rahmani, C. Jagadish, H. Tan, D. Neshev and C. De Angelis, *Adv. Phys.: X*, 2022, **7**, 2022992.
152. A. Fedotova, M. Younesi, J. Sautter, A. Vaskin, F. J. F. Löchner, M. Steinert, R. Geiss, T. Pertsch, I. Staude and F. Setzpfandt, *Nano Lett.*, 2020, **20**, 8608–8614.
153. L. Qu, L. Bai, C. Jin, Q. Liu, W. Wu, B. Gao, J. Li, W. Cai, M. Ren and J. Xu, *Nano Lett.*, 2022, **22**, 9652–9657.
154. M. R. Shcherbakov, D. N. Neshev, B. Hopkins, A. S. Shorokhov, I. Staude, E. V. Melik-Gaykazyan, M. Decker, A. A. Ezhov, A. E. Miroshnichenko, I. Brener, A. A. Fedyanin and Y. S. Kivshar, *Nano Lett.*, 2014, **14**, 6488–6492.

155. S. S. Kruk, L. Wang, B. Sain, Z. Dong, J. Yang, T. Zentgraf and Y. Kivshar, *Nat. Photonics*, 2022, **16**, 561–565.
156. G. Balasubramanian, I. Y. Chan, R. Kolesov, M. Al-Hmoud, J. Tisler, C. Shin, C. Kim, A. Wojcik, P. R. Hemmer, A. Krueger, T. Hanke, A. Leitenstorfer, R. Bratschitsch, F. Jelezko and J. Wrachtrup, *Nature*, 2008, **455**, 648–651.
157. M. R. Shcherbakov, H. Zhang, M. Tripepi, G. Sartorello, N. Talisa, A. AlShafey, Z. Fan, J. Twardowski, L. A. Krivitsky, A. I. Kuznetsov, E. Chowdhury and G. Shvets, *Nat. Commun.*, 2021, **12**, 4185.
158. G. Zograf, K. Koshelev, A. Zalogina, V. Korolev, R. Hollinger, D.-Y. Choi, M. Zuerch, C. Spielmann, B. Luther-Davies, D. Kartashov, S. V. Makarov, S. S. Kruk and Y. Kivshar, *ACS Photonics*, 2022, **9**, 567–574.
159. E. J. Murphy, *Integrated Optical Circuits and Components: Design and Applications*, CRC Press, 2020.
160. C. Wang, Z. Li, M.-H. Kim, X. Xiong, X.-F. Ren, G.-C. Guo, N. Yu and M. Lončar, *Nat. Commun.*, 2017, **8**, 2098.
161. Z. Li, B. Corbett, A. Gocalinska, E. Pelucchi, W. Chen, K. M. Ryan, P. Khan, C. Silien, H. Xu and N. Liu, *Light: Sci. Appl.*, 2020, **9**, 180.